Electronic Supplementary Material (ESI) for Analyst.

Supporting Information

Understanding Electrocatalytic Mechanisms and Ultra-Trace Uranyl Detection with Pd Nanoparticles Electrodeposited in Deep Eutectic Solvents

Arkaprava Layek[a], Sushil Patil[a,c], Ruma Gupta[a,c*], Priya Yadav[b,c], Kavitha Jayachandran[a,] D. K. Maity[c] and Niharendu Choudhury[b,c]

[a]*Fuel Chemistry Division,* [b]*Chemistry Division, Bhabha Atomic Research Centre, Trombay, Mumbai-400085, India*

[c]*Homi Bhabha National Institute, Training School Complex, Anushakti Nagar, Mumbai 400094, India*

***Corresponding Author**

*Tel: +91-22-25594188; E-mail: ruma.chandra@gmail.com (RG), and Fax: +91-22-25505151;

Table S1: Comparison of recent literature available for uranium determination employing various different techniques with the present method.

Analytical Method	Substrate	Remark	Reference
Colorimetry	Covalent Organic Framework Nanozyme	Prolong response time, complicated synthesis steps LOD = not given	1
Energy dispersive X-ray fluorescence spectrometry	Aluminum annular discs with adhesive scotch tape	Higher detection limit, severe matrix effect, complicated and sensitive maintenance needed, difficult to use for on-site monitoring	2
Lateral Fow Strips	U(VI) selective gold nanoparticle-based lateral fow strips.	Simpler, cost-effective, Biocompatible and high sensitivity due to intense plasmonic effect. LOD = 36.38nM	3
Colorimetry	Vinylphosphonic acid functionalized AuNPs	Simple, portable, on-site measurement, Need of reducing agent and stabilizer. LOD = 1.07 μM	4
Surface-Enhanced Raman Scattering	Magnetic MOF (Fe_3O_4@SiO_2@ Au)	Comparatively time-consuming synthesis, low efficiency, good sensitivity and selectivity in neutral and alkaline environments but poor result in acidic environment LOD = 1×10^{-7} M	5
Fluorescence	fluorescent sensor TPE-BSA	Expensive and complex systems with high cost of operation and maintenance LOD = 0.039 μM	6

Differential Pulse Voltammetry	Pd nanoparticles deposited on Au electrode	Simple and additive free method for synthesis of PdNPs, detection of sub-ppb concentration of Uranyl ion, advantages of high precision, reproducible stable current response, excellent sensitivity and simple equipment requirements. Low costs for experiments and maintenance, can be used as portable equipments for on-site environmental monitoring. LOD = 0.82 ppb	**Present work**

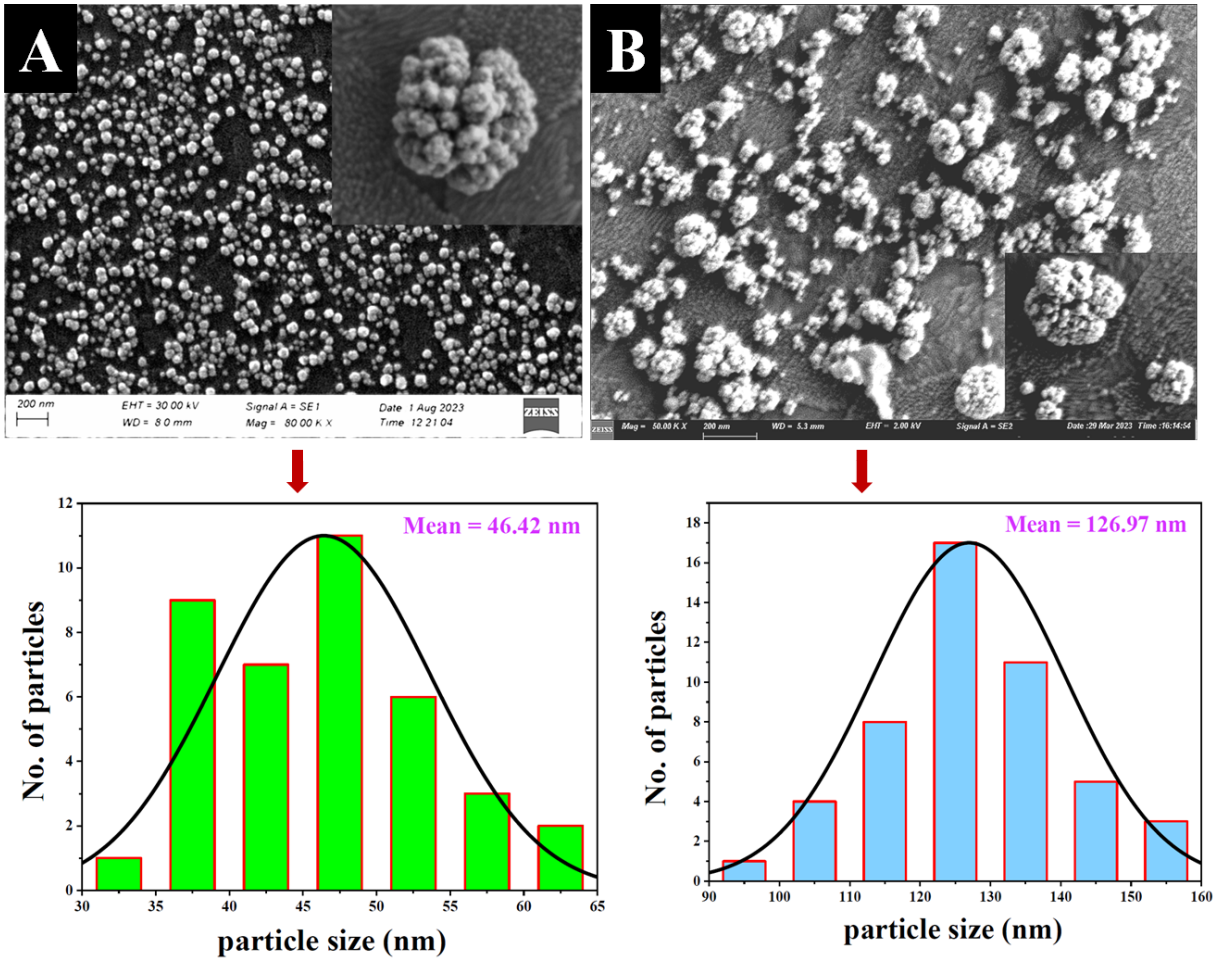

Figure S1: FESEM images of PdNPs electrodeposited A)with 5% hydration of DES andB) under heating condition

Section S1: Mechanism of different shapes of PdNPs deposition employing DES

Utilizing deep eutectic solvents (DES) as a medium for nanoparticle electrodeposition presents several benefits in contrast to traditional approaches employing standard solvents. Scheme 1 illustrates the potential mechanistic aspects influencing the formation of diverse Pd nanoparticle shapes under varying conditions. In this study, the DES employed consists of Choline chloride and urea in a 1:2 ratios, composed of natural components devoid of toxicity. This characteristic endows the electrodeposition process from DES with ecological integrity, aligning seamlessly with sustainable practices. The decreased viscosity, due to water addition and heating, inherent in DES heightens the transport of ions to the electrode surface, engendering an enhanced mass transfer phenomenon. Consequently, electrodeposition gains efficiency, potentially reducing the

energy demand for the deposition process. Furthermore, the lower viscosity and unique solvation attributes of the current DES formulation facilitate the realization of uniform particles with diminished tendencies for aggregation.Upon the addition of 5% water into the DES medium containing palladium salt, the morphology of the nanoparticles transitions from distorted spheres to cauliflower-like structures. The introduction of water into the Reline DES engages in competition with urea for hydrogen bond interaction with choline chloride. This competitive interaction induces alterations in the solvation environment around the Pd^{2+} ions. The modified solvation environment is postulated to influence growth kinetics and the favored crystallographic facets of the PdNPs, thus shaping them into cauliflower forms.Additionally, subjecting the system to a temperature of 60°C results in further changes in morphology. This phenomenon can be attributed to the elevated temperature of the reline DES, which increases the thermal energy within the system. This, in turn, boosts collision frequency and energy of the palladium precursor while reducing the overall system viscosity. As a consequence, heterogeneous rates—nucleation and growth processes in particular—accelerate.

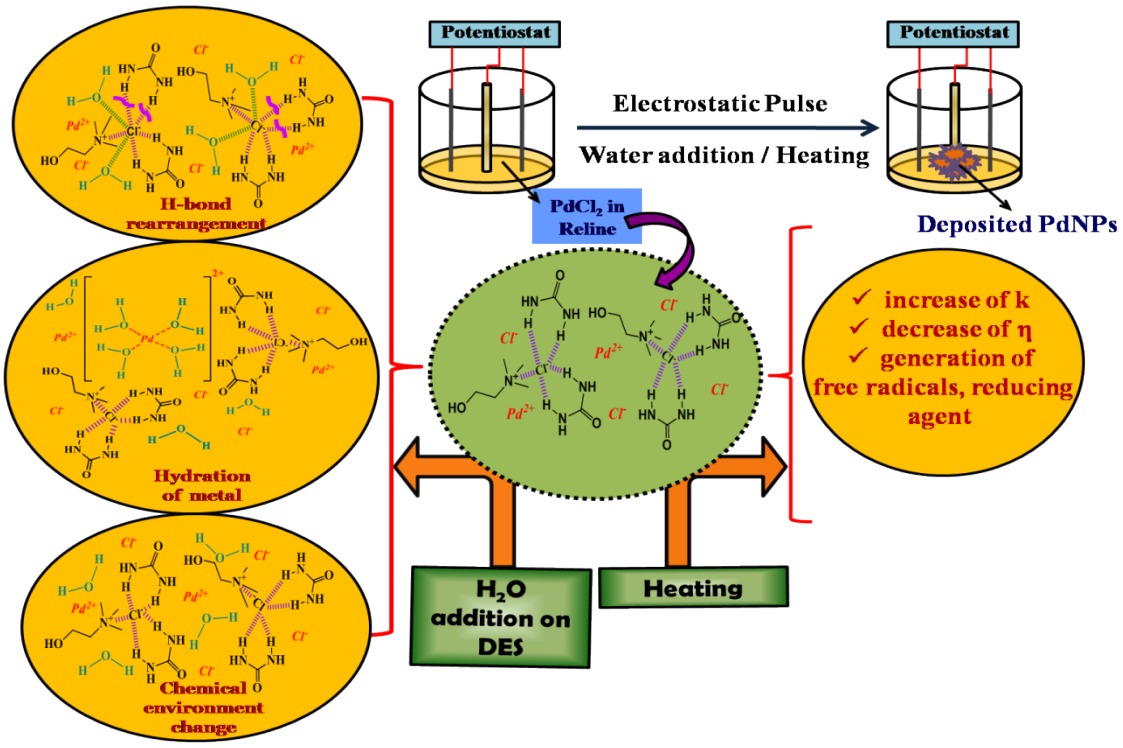

Scheme 1:Probable mechanistic aspect of getting different shape of Pd nanoparticles under different condition viz. water addition into DES and heating the DES system

The heightened reaction kinetics exerts an impact on nucleation sites, growth rates, and nanoparticle aggregation behavior, ultimately influencing their resulting shape. This potentially accounts for the observed agglomeration of particles, leading to the formation of larger, flower-like structures.By modifying the water content within the DES and applying heat, various forms of PdNPs, including those resembling flowers, were synthesized with distinct surface structures.The synthesis process was finely tuned to yield nanoparticles of different shapes and distinctive surface characteristics. This innovative method offers a versatile and efficient route for tailoring nanoparticle morphology, enabling researchers to explore a wide range of applications where specific shapes and surface structures are crucial for optimized performance and functionality.

Section S2. Determination of electrochemical active surface area

To determine the electrochemically active surface area of the three modified electrodes, cyclic voltammetry experiments were conducted using a 5 mM potassium ferricyanide solution as the redox probe. In cyclic voltammetry studies, the current associated with the electrochemical reaction occurring at the electrode surface, particularly when it is limited by mass transfer, can be quantified using the Randle-Sevick equation.

$$I_p^c = 2.69 \times 10^5 n^{\frac{3}{2}} D^{\frac{1}{2}} A C_o \nu^{\frac{1}{2}}$$

where A is the electrochemical active area, D is the diffusion coefficient, C is the bulk concentration of ferricyanide, n is the number of electrons transferred and □ is the scan rate[7]. In the case of a diffusion-controlled process, when we plot the current peak (I_{pc}) against the square root of the scan rate ($\nu^{1/2}$), the resulting graph will exhibit a linear relationship. From the slope of this linear plot, we can determine the value of parameter A. This is possible because we have precise knowledge of the diffusion coefficient of ferricyanide, which is 8.9×10^{-6} cm^2/s.

For the electrochemically active surface area (EASA), the bare gold electrode had a value of 0.031 cm^2. In contrast, when PdNPs were deposited on the gold electrode using a room temperature deposition electrochemical solution (DES), the EASA increased to 0.112 cm^2. When PdNPs were deposited under conditions involving 5% hydration of the DES, the EASA further increased to 0.141 cm^2. Lastly, when the deposition was carried out with heating, the EASA was determined to be 0.10 cm^2.

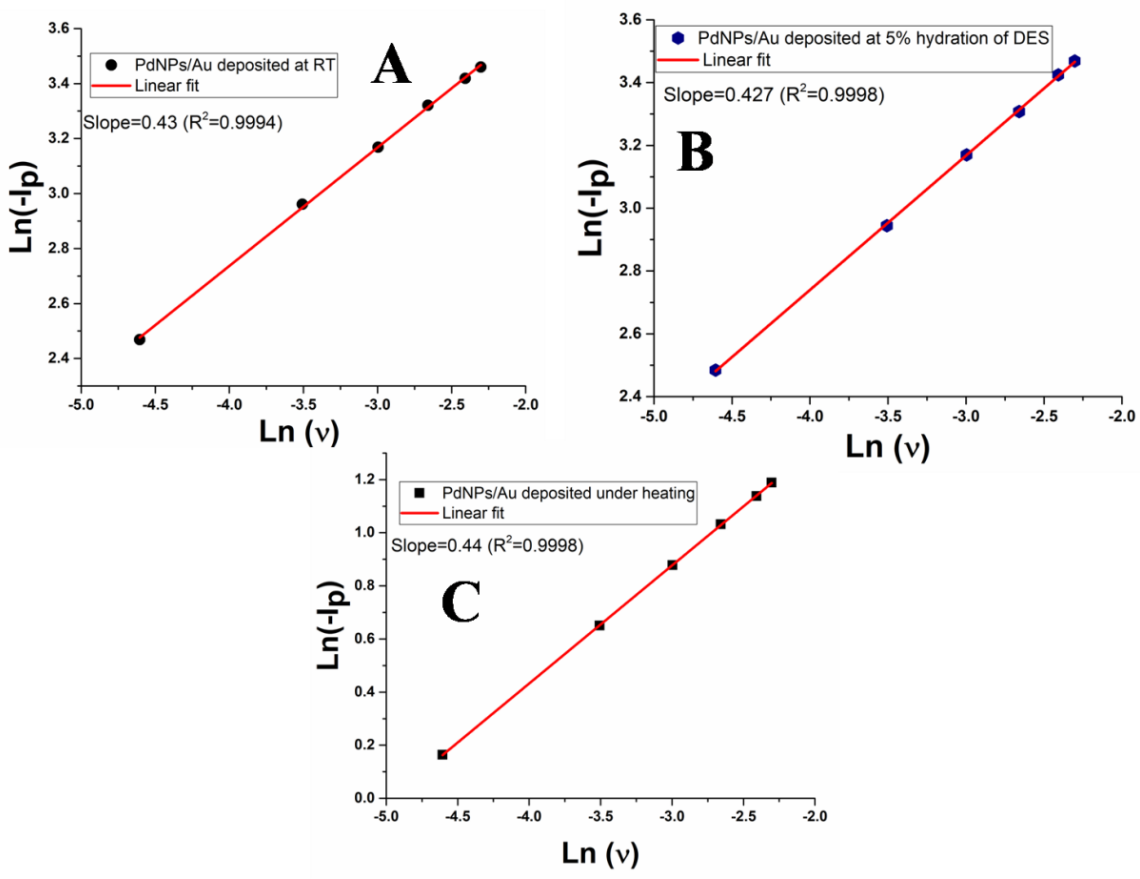

Figure S2: The variation of Ln(-I_p) with Ln(ν) observed in PdNPs/Au electrode deposited A)at RT B) with 5% hydration of DES andC) under heated conditionin the system 5 mM U(VI) in saturated Na_2CO_3 solution (I_{pc} = cathodic peak current, ν = scan rate)

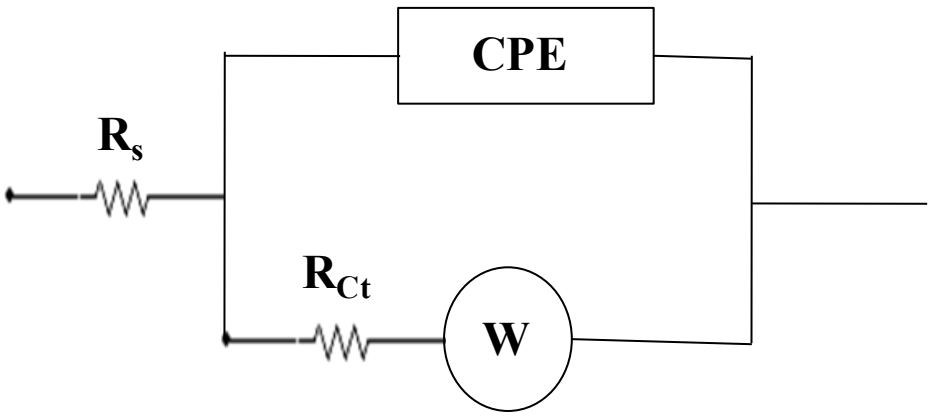

Figure S3. Equivalent circuit used for fitting the impedance.

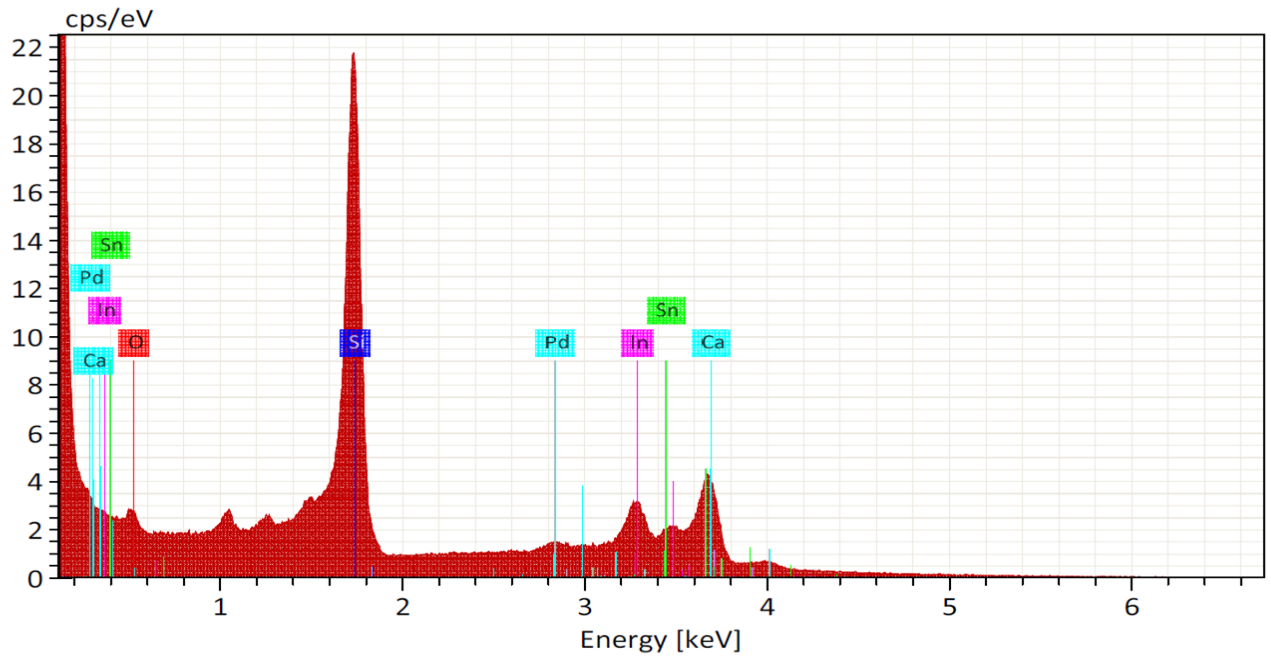

Figure S4. EDS spectra of PdNPs deposited at ITO substrate after equilibration with solution containing UO_2^{2+}

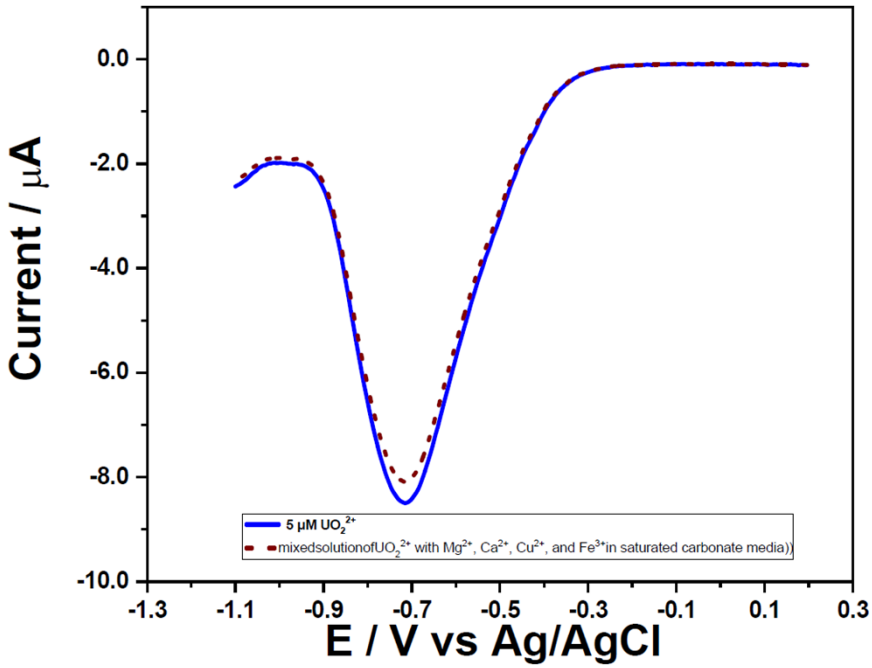

Figure S5. DPV of 5 µM UO_2^{2+} and mixed solution of UO_2^{2+}, Ca^{2+}, Cu^{2+}, , Mg^{2+}, and Fe^{3+} (5 µM each) in saturated carbonate media recorded at PdNPs/Au electrode

Table S2: Average structural parameters of uranyl(VI/V) carbonate complexes with the 3 Na^+ ions

Parameters	Calculated		Reference[8]	
	$Na_3[UO_2(CO_3)_3]^-$	$Na_3[UO_2(CO_3)_3]^{2-}$	$Na_3[UO_2(CO_3)_3]^-$	$Na_3[UO_2(CO_3)_3]^{2-}$
U=O (Å)	1.81	1.88	1.81	1.88
U-O_c (Å)	2.45	2.54, 2.56	2.46	2.55
U-C (Å)	2.92	3.00	2.93	3.01
U-Na (Å)	3.78	3.74	3.96	3.94

Reference:

1. L. Zhang, G. P. Yang, S. J. Xiao, Q. G. Tan, Q. Q. Zheng, R. P. Liang and J. D. Qiu, *Small*, 2021, **17**, 2102944.
2. K. Sanyal and N. L. Misra, *Spectrochimica Acta Part B: Atomic Spectroscopy*, 2019, **155**, 44-49.
3. D. Quesada-González, G. A. Jairo, R. C. Blake, D. A. Blake and A. Merkoçi, *Scientific Reports*, 2018, **8**, 16157.
4. L. Zhang, D. Huang, P. Zhao, G. Yue, L. Yang and W. Dan, *Spectrochimica Acta Part A: Molecular and Biomolecular Spectroscopy*, 2022, **269**, 120748.
5. N. Wang, J. Du, X. Li, X. Ji, Y. Wu and Z. Sun, *Analytical Chemistry*, 2023, **95**, 12956-12963.
6. N. Lin, W. Ren, J. Hu, B. Gao, D. Yuan, X. Wang and J. Fu, *Dyes and Pigments*, 2019, **166**, 182-188.

7. A. J. Bard, L. R. Faulkner and H. S. White, *Electrochemical methods: fundamentals and applications*, John Wiley & Sons2022.
8. A. Ikeda, C. Hennig, S. Tsushima, K. Takao, Y. Ikeda, A. C. Scheinost and G. Bernhard, *Inorganic chemistry*, 2007, **46**, 4212-4219.